Plasma Chemistry and Plasma Processing, Vol. 11, No. 1, 1991

Comparison of Temperature and Work Function Measurements Obtained with Different GTA Electrodes

Masao Ushio[1], Alber A. Sadek,[1]
and. Fukuhisa Matsuda[1]

Received July 25, 1989; revised April 6, 1990

This work was carried out on one standard electrode (W-ThO_2) and other electrodes developed by additions of La_2O_3, CeO_2, and Y_2O_3. The effect of rare-earth metal oxides on GTAW electrode phenomena, concerning electrode temperature, emissivity, and work function, was analyzed and compared from the point of view of those oxides' behavior during arcing. The experimental results indicate that the electrode temperature, emissivity, and work function strongly depend on the behavior of the rare-earth metal oxides during arcing. The investigation demonstrates good stability of La_2O_3 during arcing compared with the other oxides. The temperature distributions along the electrode axis of these electrodes were measured by using infrared pyrometer and grooved electrodes. The W-La_2O_3 electrode showed the lowest temperature values, followed by W-CeO_2 and W-ThO_2 electrodes in that order. Also W-La_2O_3 electrodes have a higher emissivity and lower work function, followed by W-CeO_2 and W-ThO_2 electrodes in that order.

KEY WORDS: Arc electrodes; rare-earth additions; thermionic emission; experimental.

1. INTRODUCTION

Recent arc plasma technology, such as robotic welding, plasma spraying, thermal plasma chemistry, etc. demands superior stability and reliability for long-term operation of gas-tungsten arc (GTA) electrodes.

Tungsten electrodes activated with thoria (ThO_2) and zirconia (ZrO_2) are used for their good characteristics in arc starting.[1,2] However, these electrodes lack arc stability and show high erosion rates. It is desirable to satisfy these practical and technical requirements.

[1] Welding Research Institute, Osaka University, Mihogaoka, Ibaraki, Osaka 567, Japan.

0272-4324/91/0300-0081$06.50/0

Although considerable work has been done on describing electrode erosion rates for specific experimental conditions[3-5], the number of parameters of influencing this erosion is so large that it is in general not possible to predict erosion rates under different experimental conditions. Heberlein[6] summarized the factors which affect the electrode erosion and concluded that a better understanding of these phenomena will lead to longer life of plasma torches. Moreover, he enumerated the major areas requiring attention of researchers. In that list the electrode effects are listed first not because research in this area will have the largest impact on any one application, but because it will influence the largest number of applications. Pfender[7] also showed that there is a direct link between the method of stabilizing the arc column and the options available for the design of arc devices or the electrode materials.

In general, electrode erosion resistance and arc stability can be improved if new activators are found or suitable electrode designs are developed.[8] The required electrode features include easy arc starting, lower consumption of electrode materials to ensure arc stability, arc stability with changes in electric power, etc.

In the previous study,[9] the superiority of the arc characteristics achieved by tungsten electrodes activated by La_2O_3, Y_2O_3, and CeO_2 compared with those of the ThO_2 tungsten electrodes is obvious. The W-La_2O_3 electrodes had the best properties.

In order to clarify the differences between those oxides and their effects on arc characteristics, electrode temperature, emissivity, and work function, it is necessary to make a study of the comparable metallurgical characteristics and the behavior of those oxides during arcing, with special consideration of the electrode temperature of measurements during arcing as well as of the local surface emissivity changes and the electrode work function measurements.

2. EXPERIMENTAL PROCEDURES

The electrodes investigated in this work were produced by the conventional powder metallurgy process as centerless ground rods 2.4 and 3.2 mm in diameter. The electrodes so produced have the composition indicated in Table I. The welding system was a conventional constant current type, with a negative direct current in the electrode and a copper water-cooled anode. A constant arc length of 3 mm and torch orientation perpendicular to the anode were used throughout the series of tests.

Specimens were prepared for metallographic examination by means of hand grinding through No. 1500 emery papers and polishing with fine alumina. Polished specimens were electrolytically etched in a 10% solution

Table I. Oxide Content in Tungsten Electrode Produced

Electrode		Oxide content (%)
Thoriated tungsten	(ThO_2-W)	2
Yttriated tungsten	(Y_2O_3-W)	2
Ceriated tungsten	(CeO_2-W)	2
Lanthanized tungsten	(La_2O_3-W)	2

of 1 N NaOH for SEM observation. During the electrolytic etching, the voltage was set at 30 V for 30 sec. This aids in the delineation of the morphological changes of the oxide shape after arcing. To observe the microstructure and the recrystallized grains after arcing, Murakami's reagent (a solution of 10 g K_3 $Fe(CN)_6$, 10 g KOH, and 100 ml water) was used. It was applied by swabbing for 5-10 sec.

3. EXPERIMENTAL RESULTS

It will not be appropriate to report, in this short discussion, the details of all experimental results. We shall restrict ourselves to a brief summary of the most important facts and parameters.

3.1. Behavior of Rare-Earth Metal Oxides during Arcing

The electrodes were arced with a constant arc current (200 A) for time intervals from 1 sec to 1 h of arcing in pure argon to observe the metallurgical changes and the behavior of oxides. Figure 1 shows the EDX line analysis of lanthanum, thorium, and cerium after 30 and 60 min of arcing, for W-LA_2O_3, W-ThO_2, and W-CeO_2 electrodes, respectively. Note that in the case of W-Y_2O_3 electrodes it is difficult to record the EDX line analysis due to the interference between the tungsten and yttrium peaks. It is obvious that the distribution of both La_2O_3 and ThO_2 changed and concentrated at some places determined by the temperature distribution, suggesting that La_2O_3 and ThO_2 may migrate and accumulate at regions near the tip, while at the tip the vaporization rate of those oxides is much higher than that of the migration process. On the other hand, it can be noted that the CeO_2 has a uniform distribution throughout the electrode tip without concentration peaks, suggesting that the migration and vaporization rates of CeO_2 are much higher than that of the other oxides.

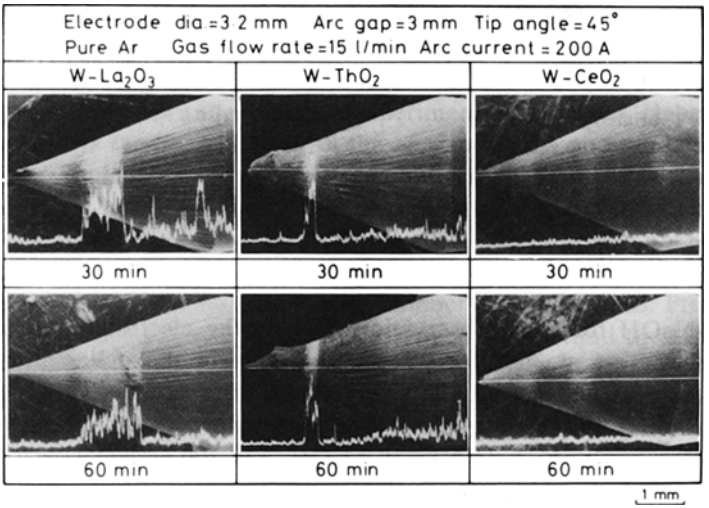

Fig. 1. Appearance of electrode surface and oxide distribution throughout the electrode tip of W-La_2O_3, W-ThO_2, and W-CeO_2.

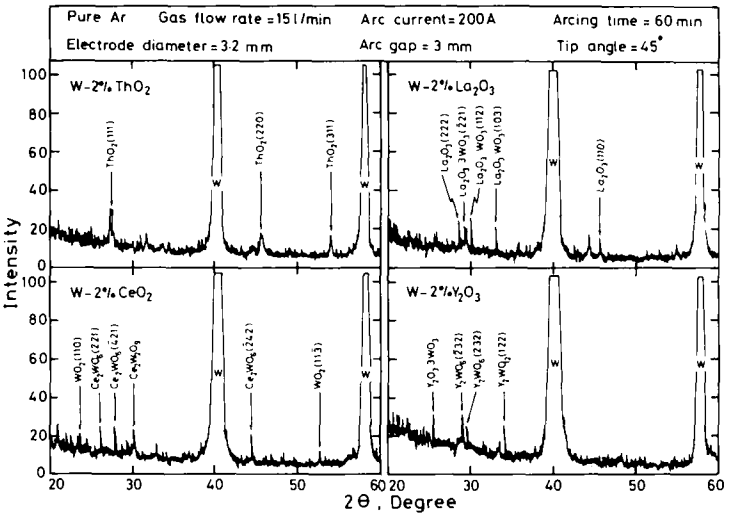

Fig. 2. X-ray analysis of different electrode tips after arc burning.

Electrodes were investigated by X-ray diffraction analysis after arcing, and the results are shown in Fig. 2. Generally the rare-earth metal oxides react with tungsten forming tungstate or oxytungstate. The melting points of those tungstates and oxytungstates are lower than that of oxides or tungsten. However, in the case of W-ThO_2 electrode no tungstate or oxytungstate is detected. Thus the ThO_2 is believed to react with tungsten forming pure Th during arcing.[10-13]

The collected data for physical and thermodynamic properties and the experimental observations for oxide behavior are given in Table II. Note that only CeO_2 was reduced to Ce_2O_3 after sintering in pure hydrogen

Table II. Summary of Oxides Behavior

Type of oxides	ThO_2	La_2O_3	CeO_2	Y_2O_3
Melting point (K)	3323 (Th: 2028)	2490 (La: 1193)	2873 (Ce: 1071)	2708 (Y: 1799)
Heat of decomposition (kJ)	1227.6	1244.7	(523.4)	1271.1
Type of oxides after sintering	ThO_2	La_2O_3	Ce_2O_3 (M.P. 1963 K)	Y_2O_3
Reaction with tungsten	Reduction of ThO by W occurs forming pure Th	Forms tungstate (M.P 2073 K) and oxytungstate (M.P >1773 K)	Forms tungstate (M.P. 1363 K)	Forms tungstate (M.P. 1743 K) and oxytungstate (M.P. >2473 K)
Oxide behavior	1. Diffusion of Th atoms to the electrode surface 2. Vaporization of the Th from the electrode surface	1. Migration of La_2O_3 occurs from the center to the electrode tip 2. Vaporization of La_2O_3 from the electrode surface	1. Migration rate throughout the electrode edge is higher than from the center to the electrode tip 2. Vaporization of CeO_2 from the electrode surface	1. Very low migration and vaporization rates
Stability of oxides	Lower stability	Higher stability	Reasonable stability	High stability

atmosphere. This new type of oxide has the lowest melting point among those oxides. Also a schematic illustration of the suggested migration mechanism and the different behavior of oxides accompanied by the temperature distribution values throughout the electrode tip after 30 min of arcing (as will be shown later) are shown in Fig. 3. Moreover, the oxide distribution inside the electrode, after arcing, is represented schematically case by case and the following conclusions are reached:

1. In the case of rare-earth metal oxides their tungstates and oxytungstates melt and migrate from the lower-temperature zone to the higher-temperature zone along the grain boundaries (which have a longitudinal shape) due to capillary action. The migration rate increases considerably with increasing temperature gradient and depends upon the melting point of the tungstates or oxytungstates. Also, as the migrated particles travel up the temperature gradient, they are accelerated and increase in size. A detailed investigation and analysis of the migrating particles throughout the electrode tip was made and a summary of the results is conntained in Fig. 4. It is apparent that there is a concentration gradient of W and La set up throughout the migrated particles as follows: At the bulk of the electrode and far from the tip, the ratio between W concentration and La concentration is almost the same (1:1 oxytungstate), but when moving in the tip direction the relative La concentration becomes higher. At the tip, vaporization of La_2O_3

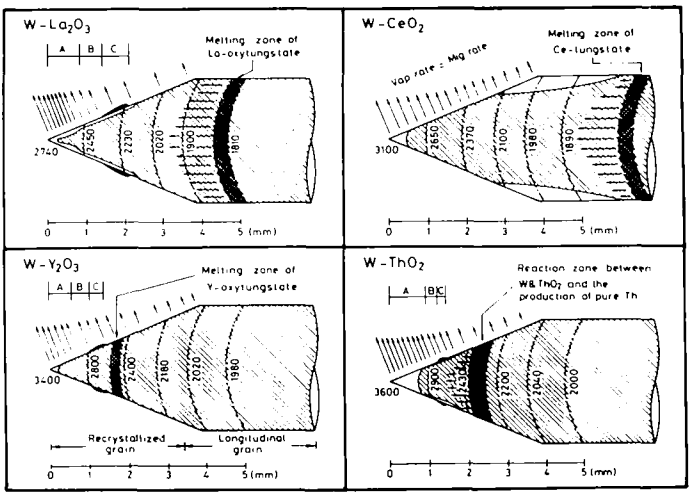

Fig. 3. Schematic illustration of the oxide distribution and behavior accompanied by the temperature distribution along the electrode axis. Hatched areas represent the oxide remaining after operation, and the arrows represent the oxide vaporization.

$W\text{-}La_2O_3$ (2%) Electrode dia = 3.2 mm
Pure Ar Gas flow rate = 15 l/min
Arc current = 200 A Arc gap = 3 mm
Tip angle = 45° Arcing time = 60 min

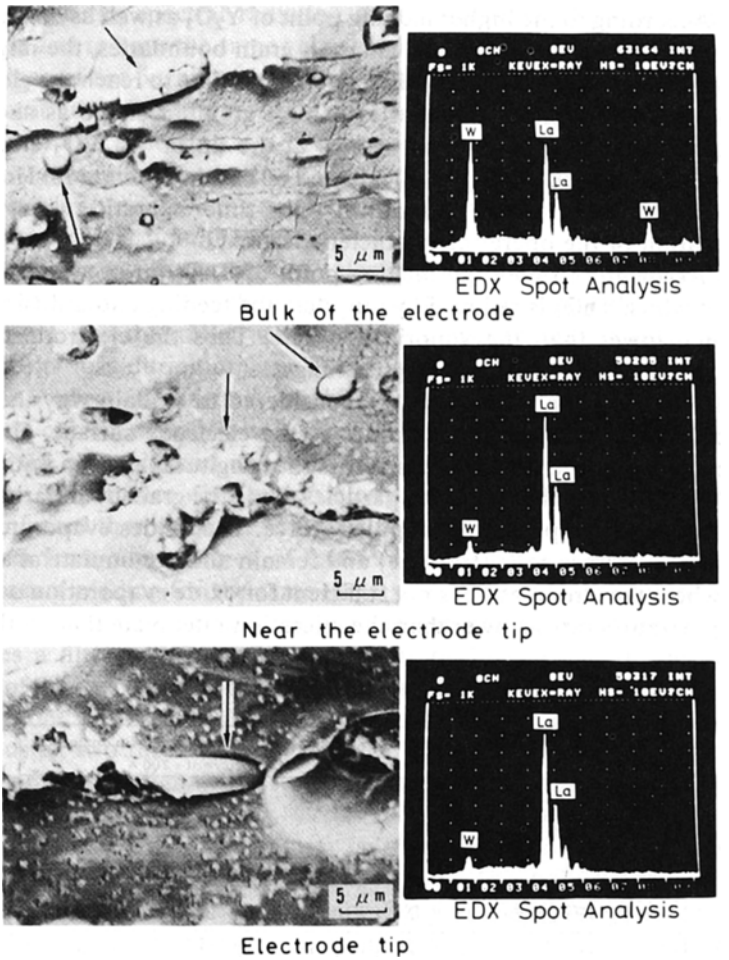

Fig. 4. EDX line analysis of the migrated particles throughout the $W\text{-}La_2O_3$ electrode.

occurred. It is inferred from this observation that the rate-limiting process is probably dissolution kinetics at the leading interface of the particles.

2. The highest migration rate among those oxides is shown by Ce_2O_3, which has a lower melting point (even for the oxide itself and for the tungstate). This oxide tungstate easily migrates and is continuously fed to the electrode tip. Thus the consumption rate of the oxide is much higher.

3. The stability of La_2O_3 was related to the slightly higher melting point of the oxide as well as of its oxytungstate compounds. Also, there is reasonable compensation between the migration and vaporization rates.

4. According to the higher melting point of Y_2O_3 as well as its tungstate or oxytungstate and the shape of tungsten grain boundaries, the migration rate along the grain boundaries takes much more time to reach the electrode tip or surface. The grain boundaries exhibit granular shape as shown in Fig. 5, which shows the microstructures at the tip of W-Y_2O_3 electrodes before and after arc burning for 30 min and 60 min in pure argon. However, a rim was formed at the tip during long-time operation and led to deterioration of the operating characteristics.

5. According to the high melting point of ThO_2 and the temperature range at which ThO_2 is reduced by tungsten, the feeding and diffusion rates are much lower than the vaporization rate. Thus the electrode tip will eliminate the ThO_2 and work as pure tungsten.

6. Another phenomenon can be considered to explain why there is a high concentration area of the oxides at the electrode surface. Owing to the tip geometry, the tip edge cuts across the longitudinal grain boundaries of the tungsten, and the migrating particles along the grain boundaries reach the surface of the tip due to a capillary force. The oxides evaporate at the highest temperature zone (tip zone) and remain and accumulate at another zone, where the temperature is not sufficient for oxide evaporation or where the vaporization rate is lower than the migration rate. Note that, in the case

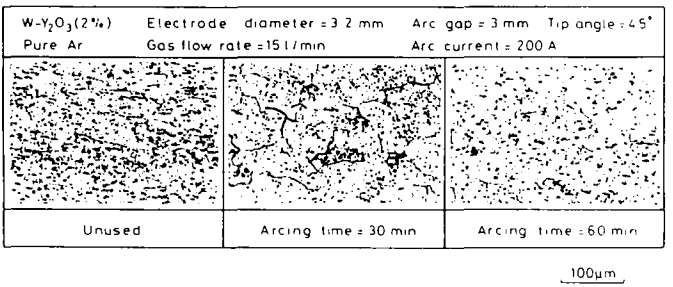

Fig. 5. Microstructure of W-Y_2O_3 electrode tip before and after arc burning.

of W-CeO_2 electrode, due to the approximately equal vaporization and migration rates no high-concentration zones are detected.

3.2. Electrode Temperature

In the case of an electrode containing oxides, the measured curve of temperature distribution shows abnormal peaks,[14] which reflects either the change in surface condition during arcing or the local concentration of oxides as showed before. The error of some measuring methods comes mainly from the spectral radiation emissivity, which was assumed to be constant and to have the same value as ohmically heated tungsten.[15,16] But in the case of arc burning, the changes of cathode surface morphology and the distribution of oxides have a very great influence on the spectral emissivity. The following is a description of the procedure and the result of a new measuring method of GTA cathode temperature, through which it is possible to measure the temperature and emissivity distributions along the electrode axis simultaneously.

In this measuring method, electrodes, 2.4 mm in diameter, were machined to contain a V-shape groove with the geometry shown in Fig. 6. The groove was then filled with graphite powder under extreme pressure to avoid its loss during arcing. The graphite powder has an emissivity of 0.97. The effect of inserted graphite on the measured temperature and electrode current density within sensible limits was assessed and found not to alter the general trend of results.

The temperature distribution along the electrode axis was measured using infrared thermometer. This type of thermometer collects the infrared radiation from a target area of 0.65 mm in diameter and converts it to a temperature reading for the same target area. The system is equipped with an InSb detector. It has been designed as a special side-looking unit which includes a filter with a wavelength range of 1.8-5.0 μm. In the infrared region of the spectrum the arc radiation has almost no effect on the measured temperature.[17] Also, the level of emissivity with a resolution of 1% can be set by using two thumbwheels. Figure 7 shows a schematic illustration of the experimental alignment used in this measuring method.

The measuring procedure was as follows:

The first step was to measure the temperature distribution along the electrode axis using the grooved electrodes filled with the graphite powder. The calibration of the infrared thermometer was then set using an emissivity value of 0.97. The temperature distribution was measured at 150 A, in pure argon at several time intervals to avoid severe melting of the tip.

The second step was to determine the local emissivity values and their changes with time, which can be attributed to the surface morphological

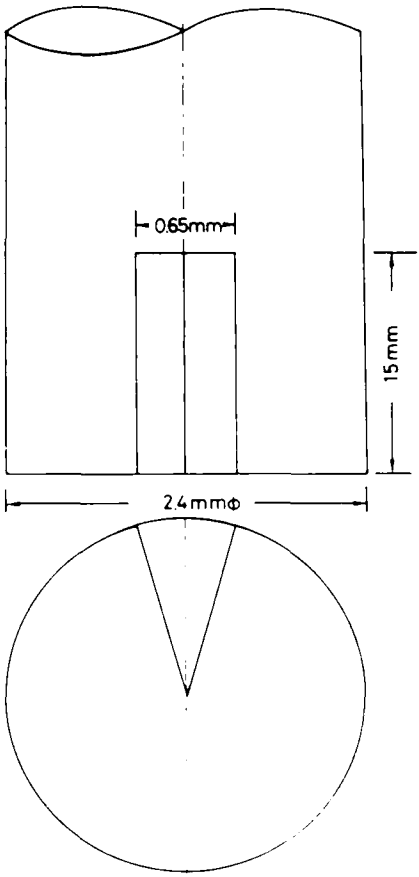

Fig. 6. Geometry of V-shape grooved electrode.

changes or to the oxide distribution, and their migration during arcing. Here, in order to have the same starting surface condition, electrodes were ground by means of hand grinding through No. 1500 emery papers, washed by acetone, and handled with care to avoid finger prints which may affect the measuring emissivity values. With the temperature distribution measured in the first step, the local emissivity can be determined by aiming the instrument at the target and adjusting the emissivity control until the meter reading is the same as that during the previously measured temperature.

The actual temperature and emissivity distribution of W-La_2O_3, W-CeO_2, and W-ThO_2 measured by this method has been tabulated and plotted in Table III and Figs. 8 and 9, respectively. It is difficult to compare these results of emissivity with those presented by earlier investigation because

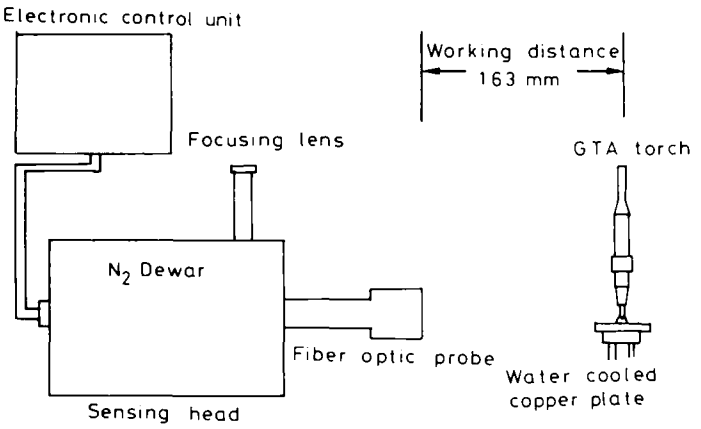

Fig. 7. Schematic illustration of the temperature measurement alignment.

the conditions under which the tests were done differ in terms of the pyrometer effective wavelength, the type of material, the surface condition for emissivity measurement, and various other factors that contribute to the variation in emissivity values.

Figure 8 is a plot of the temperature vs. the distance from the electrode tip for the investigated electrodes. From this figure it is obvious that the W-La_2O_3 electrode has the lowest temperature values, followed by W-CeO_2 and W-ThO_2. However, in this method there are no abnormal peaks, which had been observed with another method.[14] The reasons for the observed peaks can be understood from Fig. 9. It is obvious that at the location of those peaks the electrodes have higher emissivity values as in the case of

Table III. Temperature and Emissivity Values along the Electrode Tip for Several Electrodes after 30 min of Arcing at 150 A in Pure Ar

		Tip	1 mm	2 mm	3 mm	4 mm	5 mm
W-ThO_2	Temperature (K)	3613	2873	2433	2193	2063	1983
	Emissivity $\varepsilon(T)$	0.18	0.25	0.27	0.34	0.38	0.38
W-C_eO_2	Temperature (K)	3073	2673	2303	2093	1963	1893
	Emissivity $\varepsilon(T)$	0.22	0.26	0.32	0.36	0.38	0.39
W-La_2O_3	Temperature (K)	2713	2453	2223	2023	1913	1773
	Emissivity $\varepsilon(T)$	0.30	0.33	0.97	0.37	0.43	0.43

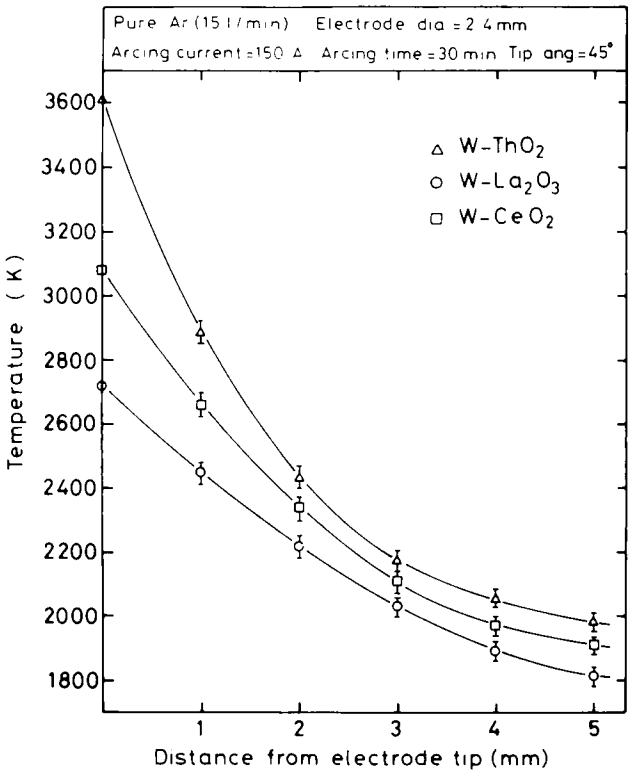

Fig. 8. Temperature distribution along the electrode axis.

the W-La_2O_3 electrode. The sudden and local change was believed to be due to the local increase of oxide at the surface and the change of surface conditions according to that. This can also be inferred from Fig. 10, which shows the temperature distribution and EDX line analysis of La along the electrode axis of ungrooved W-La_2O_3 electrode using the same measuring alignment and measuring the temperature assuming the emissivity value is constant and equal to the emissivity of tungsten. It is apparent that the location of the abnormal peaks is coincident with the concentration peaks of La_2O_3 along the electrode axis. Thus, there is much evidence suggesting that the electrode emissivity is directly linked to the oxide distribution along the electrode surface.

However, it is worth noting that, in the case of W-ThO_2 electrode, owing to the narrow concentration zone of oxides on the surface and due to our experimental limitations, the actual values of the spectral emissivity peak cannot be measured. Thus, it is shown as a dotted line and its location

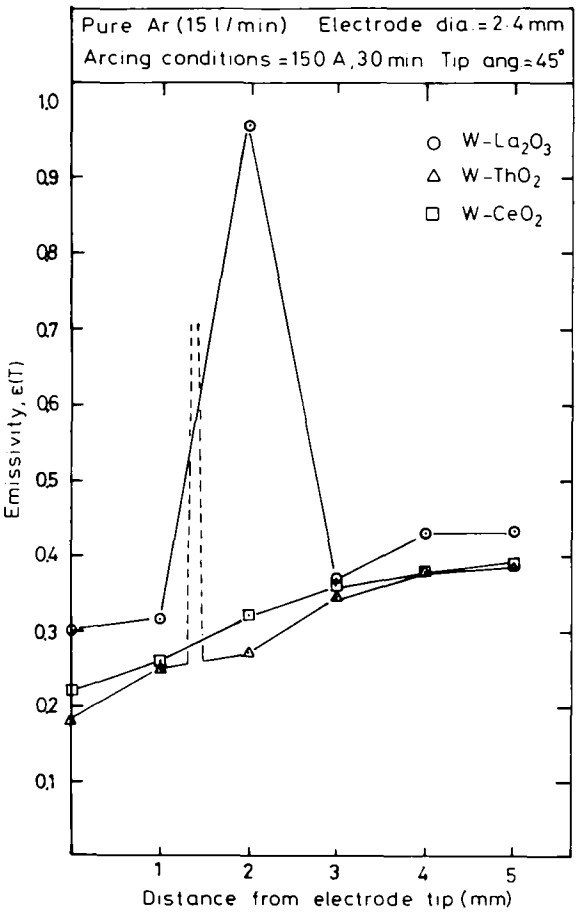

Fig. 9. Spectral emissivity distribution along the electrode axis.

was calculated after arcing by using SEM. On the other hand, in the case of the W-CeO_2 electrode, no abnormal peaks were observed due to the uniform distribution of CeO_2 along the electrode surface. The radiation emissivity of W-La_2O_3 is generally higher than that of W-CeO_2 and W-ThO_2. This result may explain why the W-La_2O_3 electrode has lower temperature values than the other electrodes.

3.3. Electrode Work Function

The electrode work function and current density were determined from photographs using the experimental alignment shown in Fig. 11 at several

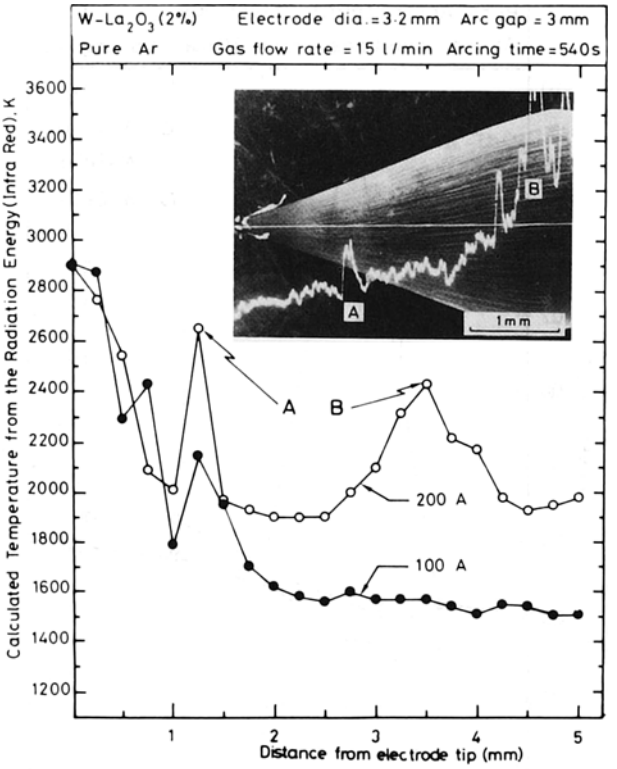

Fig. 10. Temperature distribution along ungrooved electrode measured using an infrared pyrometer assuming constant emissivity.

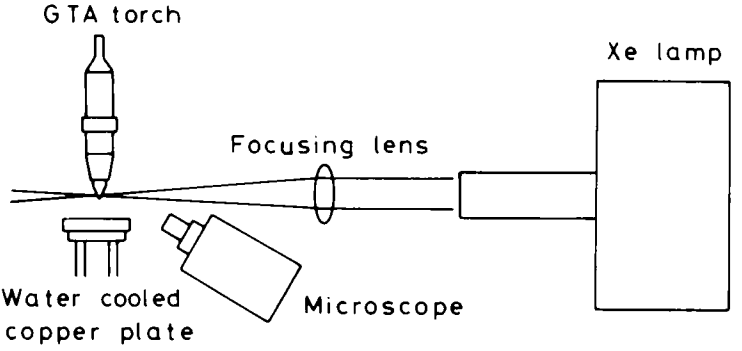

Fig. 11. Schematic illustration of direct observation alignment.

arc currents in pure argon after 5 min arcing. Figure 12 shows an example of the direct-observation photographs in the case of W-La_2O_3. Obviously, the electrode surface exhibited three characteristic zones as shown schematically in the same figure. These characteristic zones can be classified as follows: the first zone is the emitting blue arc and concentrated emission area with brightness (zone A), the second zone has a smooth surface (zone B) due to oxide vaporization which occurs without the melting of the electrode metal causing the electrode surface to become smooth, and the third zone has a rough surface due to the higher concentration of oxides in that zone (zone C). The morphological characteristics of these zones and oxide distributions in the case of W-La_2O_3 and W-ThO_2 electrodes are shown in Fig. 1. However, the size and location of these zones are dependent on the arc current which affects the temperature distribution along the electrode tip.

Assuming that the electron emission occurred in zone A, the current density at that zone was first calculated. After that, the work function was calculated using the Richardson-Dushman equation, with the temperature distribution found as previously explained:

$$J_s = AT^2 \exp(-e\Phi/KT)$$

where J_s is the current density (A/m^2), A is a constant, 1.2×10^6 ($A/m^2\ K^2$), K is Boltzmann's constant, T is the temperature (K), and Φ is the work function.

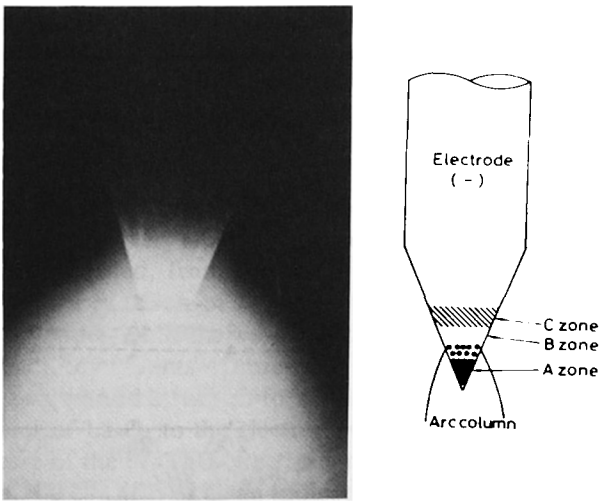

Fig. 12. Cathode surface during arc burning at various currents in pure Ar.

The results are plotted in Fig. 13, which shows the calculated current density and work function as a function of arc current for various electrodes in pure argon. It can be inferred from this figure that with increasing arc current the electrode work function also increases. That can be attributed to the increase in temperature with increasing arc current.

However, the W-La_2O_3 electrode has the lowest work function among the investigated electrodes, followed by W-CeO_2, W-Y_2O_3, and W-ThO_2 electrodes in that order. It may then be said that the superiority of the W-La_2O_3 electrode is a result of its ability to emit electrons readily.

The observed phenomena can be understood if the oxide behavior is considered during arcing as follows: The La oxide has high migration and continuous feeding rates to the electrode surface. In the case of the W-ThO_2 electrode the diffusing atoms which reach the surface are pure Th which

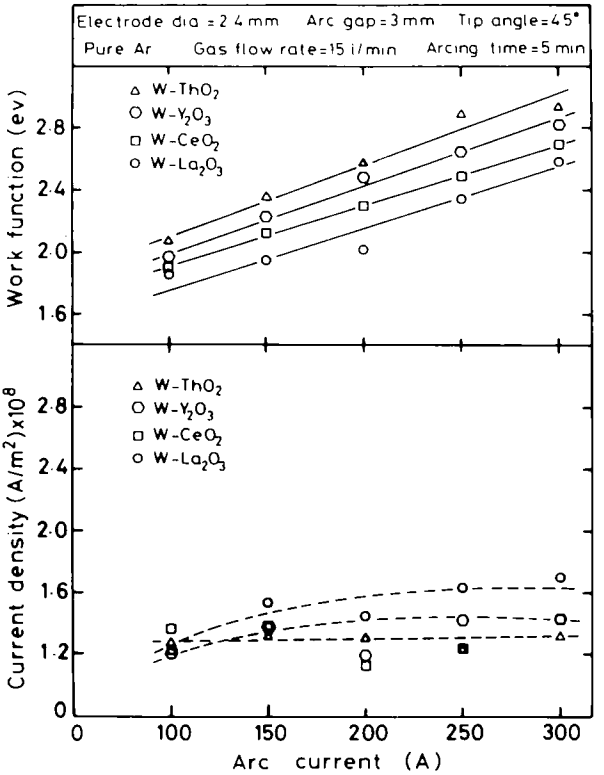

Fig. 13. Work function and current density as functions of arc current of several tungsten electrode types.

have a higher work function than La oxide. In the case of the W-Y_2O_3 electrode the migration rate of Y oxide is much lower than that of La oxide; thus, at the surface there are insufficient amounts of oxides to work as a good emitter in that case.

To observe these phenomena clearly the W-La_2O_3 and W-ThO_2 electrodes were investigated at constant arc current (200 A) for several arcing times and the work function was calculated. The results are shown in Fig. 14 for W-La_2O_3 and W-ThO_2 electrodes.

It is apparent that in the case of W-La_2O_3 electrode the change in electrode work function is small and can be considered to have a constant value (~2.1 eV). Note that the current density changes with time while the work function is approximately constant. This can be understood from Fig. 15 which shows the changes in the area of the emitting zone and the temperature of the electrode tip as functions of arcing time. Also, it shows the average volume fraction of La oxide for the three arcing periods with a schematic illustration of oxide distribution at the electrode tip. It can be inferred that:

1. During the initial phase of the arcing period, the amount of La_2O_3 decreased owing to the arc starting phenomena. This led to an increase of the area of the emitting zone which consequently decreased the current density.

2. After that the La_2O_3 reacted with tungsten-formed La tungstate and oxytungstate which have lower melting points. These new compounds migrated to the electrode tip and led to an increase in the amount of La_2O_3 content at the tip which consequently decreased the area of the emitting zone and increased the current density.

3. After a long time the vaporization of La_2O_3 from the tip increased and led to a decrease of the residual amounts of oxide at the tip and consequently increased the area of the emitting zone and increased the current density.

4. The electrode tip temperature increases slightly with increasing arcing time, resulting in very small changes in the calculated work function.

It can be concluded, from the trend exhibited previously, that the current density is a function of the migration and vaporization rates of rare-earth metal oxides, while the work function is a function of the electrode temperature and the amounts of rare-earth metal oxides on the electrode surface. This is supported by the uniform migration rate and the continuous feeding behavior of La_2O_3 to the electrode tiff during arcing. On the other hand, in the case of the W-ThO_2 electrode the work function increase with arcing time can be considered as an indication of the lower migration rate of ThO_2 (or the lower diffusion rate of pure Th) to the electrode tip which, therefore, operates as pure tungsten.

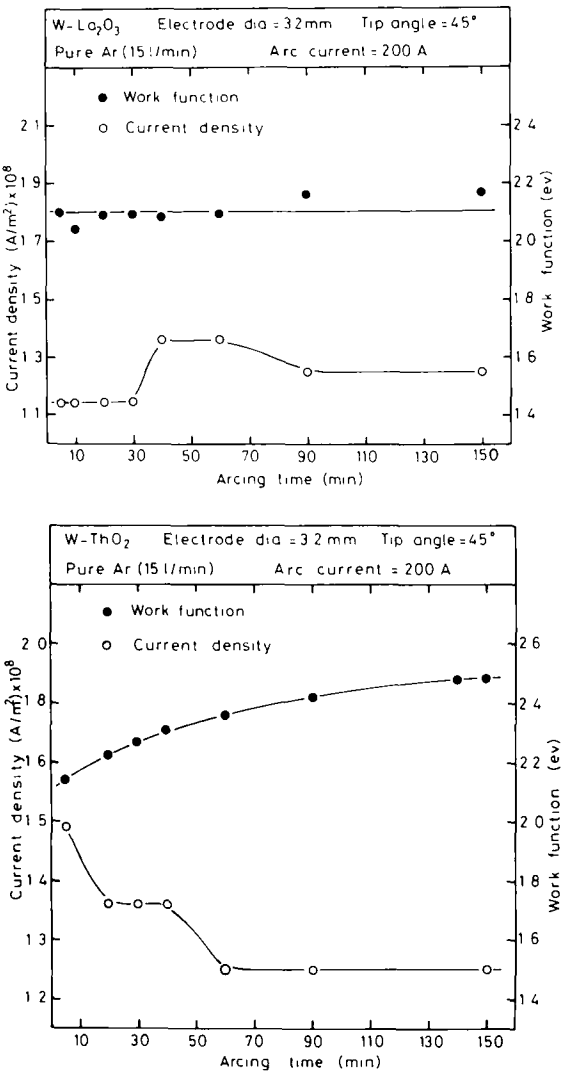

Fig. 14. Changes in work function and current density as a function of arcing time.

4. CONCLUSIONS

This study has been carried out to investigate the behavior of rare-earth metal oxides in tungsten electrodes during arcing compared with ThO_2 and to observe their effects on electrode temperature, emissivity, and work function. The main conclusions drawn from the experimental data are:

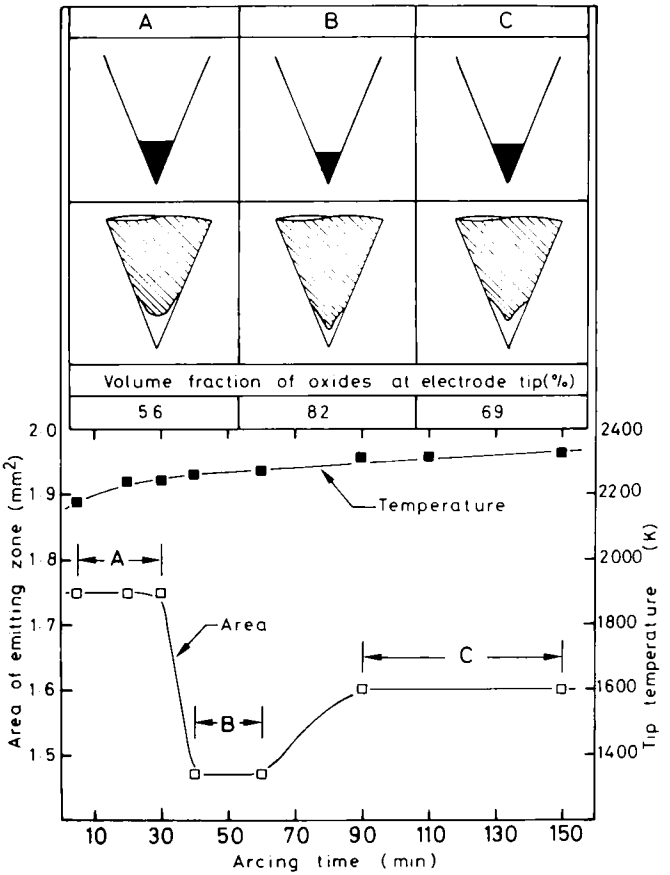

Fig. 15. Effect of arcing time on electrode tip temperature and the area of emitting zone in relation to the volume fraction of oxides at the electrode tip.

1. The Th oxide reacts with tungsten, forming pure Th. The pure Th diffuses with small amounts from the bulk to the edge of electrode and then evaporates from the electrode surface.

2. Rare-earth metal oxides react with tungsten, forming tungstates and oxytungstates. These tungstates or oxytungstates melt and migrate from the lower-temperature zone to the higher-temperature zone. The differences in their migration rates may be attributed to their melting points.

3. The tungsten electrode activated with La_2O_3 showed the lowest temperature values, followed by W-CeO_2 and W-ThO_2 in that order. Also W-La_2O_3 electrodes have a higher emissivity and lower work function, followed by W-CeO_2 and W-ThO_2 electrodes in that order.

4. The behavior of rare-earth metal oxides during arc burning is the most important factor in determining the electrode's operating characteristics, temperature, work function, electron emission, and electrode stability. Thus, an oxide that has high migration and continuous feeding rates, like La_2O_3, shows a lower work function compared with that of another oxide which has a lower migration rate, like Y_2O_3. In other words, the formation of a low-melting-point, low-work-function La tungstate and oxytungstate at the electrode tip, contrasted to the formation of a high-melting point, high- work-function Th in the case of the ThO_2-doped electrode, calls for operating the ThO_2-doped electrode at a higher temperature and work function.

ACKNOWLEDGMENT

The authors would like to express their appreciation to Toho Kinzoku Co., Ltd. for the production of the many kinds of electrodes, and to Hitachi Seiko Ltd. for valuable help with the experiments.

REFERENCES

1. L. P. Winsor and R. R. Turk, *Weld. J.* **36**, 113 (1957).
2. N. A. Chapin, J. D. Cobine, and C. J. Gallagher, *Weld. J.* **30**, 529 (1951).
3. M. G. Fey and J. McDonald, A, I.Ch.E. Plasma Processing Symposium, 1976.
4. A. E. Guile, *IEE Rev.* **118**, 1131 (1971).
5. A. E. Guile and B. Juttner, *IEEE Trans. Plasma Sci.* **PS8/3**, 259 (1980).
6. J. V. R. Heberlein, *Plasma Processing and Synthesis of Materials*, J. Szekely and D. Apelian, eds., North-Holland, New York (1984), Vol. 30, p. 101.
7. E. Pfender, *Plasma Processing and Synthesis of Materials*, J. Szekely and D. Apelian, eds., North-Holland, New York (1984), Vol. 30, p. 13.
8. M. Ushio, *Pure Appl. Chem.*, **60**, 809 (1988).
9. M. Ushio, A. A. Sadek, and F. Matsuda, IIW Asian Regional Welding Congress, Australia, 1988, Vol. 2, p. 989.
10. G. V. Samsonov, *The Oxide Handbook*, 2nd edn., IFI/Plenum, New York (1982).
11. S. W. H. Yih and C. T. Wang, *Tungsten: Sources, Metallurgy, Properties and Applications*, Plenum Press, New York (1979).
12. C. J. Smithelles, *Tungsten: A Treatise on Its Metallurgy, Properties and Applications*, 3rd edn., Chapman and Hall, London (1952).

13. G. D. Rieck, *Tungsten and Its Compound*, 1st edn., Pergamon Press, Oxford (1967).
14. F. Matsuda, M. Ushio, and H. Fujii, *Trans Jpn. Weld. Res. Inst.* **15**, 7 (1986).
15. K. Kudo, *The Fundamental and Method of Dispersion of Light*, Ohm-sha, 1980, (in Japanese).
16. J. C. Devos, *Physica* **20**, 669 (1954).
17. A. V. Pustogarov, *Variation of Electrode Temperature in the Plasma Torch*, Nauka, Novosibirsk (1977).